Available online at www.sciencedirect.com
SCIENCE DIRECT®
Bioorganic & Medicinal Chemistry 14 (2006) 479–491
Bioorganic & Medicinal Chemistry

Novel platinum(II) and palladium(II) complexes with cyclin-dependent kinase inhibitors: Synthesis, characterization and antitumour activity

Lucie Szűčová,[a] Zdeněk Trávníček,[a,b,*] Marek Zatloukal[b] and Igor Popa[b]

[a]*Department of Inorganic Chemistry, Palacký University, Křížkovského 10, CZ-771 47 Olomouc, Czech Republic*
[b]*Laboratory of Growth Regulators, Palacký University & Institute of Experimental Botany AS CR, Šlechtitelů 11, CZ-783 71 Olomouc, Czech Republic*

Received 16 May 2005; revised 18 July 2005; accepted 16 August 2005
Available online 28 September 2005

Abstract—The Pt(II) and Pd(II) complexes of the types *cis*-$[Pt(L_1)_2Cl_2]\cdot H_2O$ (**1**), *cis*-$[Pt(L_2)_2Cl_2]\cdot 3H_2O$ (**2**), *trans*-$[Pd(L_1)_2Cl_2]\cdot H_2O$ (**3**), *trans*-$[Pd(L_2)_2Cl_2]\cdot H_2O$ (**4**), *trans*-$[Pd(L_3)_2Cl_2]\cdot 2DMF$ (**5**) and *trans*-$[Pd(L_4)_2Cl_2]\cdot 2DMF$ (**6**) ($\mathbf{L_1}$–$\mathbf{L_4}$ = cyclin-dependent kinase inhibitors derived from 6-benzylamino-9-isopropylpurine) have been prepared and characterized. The complexes have been studied by elemental analyses, conductivity measurements, ES+ MS, FT-IR, ^{1}H, ^{13}C and ^{195}Pt NMR spectra, differential scanning calorimetry and thermogravimetric analysis. The molecular structures of $\mathbf{L_1}$, *trans*-$[Pd(L_3)_2Cl_2]\cdot 2DMF$ (**5**) and *trans*-$[Pd(L_4)_2Cl_2]\cdot 2DMF$ (**6**) have been determined by single crystal X-ray analysis. The complexes have been tested in vitro due to their presumable anticancer activity against the following human cancer cell lines: K-562, MCF7, G-361 and HOS. Satisfying results were obtained for the complex **1** with IC_{50} values of 6 μM acquired against G-361 as well as against HOS cell lines. The lowest values of IC_{50} were achieved for the complexes **3** and **4** against MCF 7 cell line with IC_{50} 3 μM (for **3**) and also 3 μM (for **4**).

1. Introduction

The discovery of antineoplastic effects of *cis*-(diammine)-(dichloro)platinum(II) (*Cisplatin*) in 1961,[1,2] led to the progressive development of *cisplatin*-like complexes.[3] The complexes structurally analogous to *Cisplatin*, for example, (1,2-cyclohexanediammine)-(oxalato)platinum(II) (*Oxaliplatin*)[4] or *cis*-(diammine)-(1,1-cyclobutanedicarboxylato)platinum(II) (*Carboplatin*),[5] were prepared and their anticancer effects were studied. Although *Cisplatin*, *Oxaliplatin* and *Carboplatin* have been used as effective cancer treatments, some toxic side effects and natural resistance have still remained. It was found that the substitution of NH_3 groups in *Cisplatin* by primary (especially cyclic or aromatic) amines could lead to the preparation of anticancer substances, which are less toxic.[6,7] Subsequently, *cis*- and *trans*-$[Pt(L)_2Cl_2]$ complexes have been prepared, where L = pyridine, lutidine and picoline derivatives,[7,8] anilines,[9] pyrazole,[10] benzimidazole derivatives[11] and many others. Recently, the complex of the type *cis*-$[Pt(Boh)_2Cl_2]\cdot 3H_2O$, where Boh = 2-[(3-hydroxypropyl)-amino]-6-benzylamino-9-isopropylpurine (*Bohemine*), has also been studied and its cytotoxic activity has been determined.[12] Some *trans*- and *cis*-$[Pd(L)_2Cl_2]$ complexes were also prepared and characterized, where L = inosine, guanosine,[13,14] substituted triazolo-pyrimidines[15] or pyrazole derivatives,[10] as well as some *trans*-$[Pd(L)_2Cl_2]$ complexes with L = adenosine or xanthosine.[14] For a long time, *cis*-configuration was considered to be responsible for the anticancer activity of Pt(II) and Pd(II) complexes[6] but later, *trans*-$[Pt(L)_2Cl_2]$ complexes, where L = pyridine derivatives, were published and it was stated that they show anticancer effects despite the *trans*-configuration.[7,16,17]

Organic substances with 6-benzylaminopurine moiety, belonging to a group of compounds called cytokinins, have been studied since 1960s. These compounds are able to influence plant cell division.[18] On the other hand, 2,6,9-trisubstituted purines have been intensively studied since the 1990s due to the fact that some of them strongly inhibit cyclin-dependent kinases (CDKs),[19] that is,

Keywords: Platinum(II); Palladium(II); Cyclin-dependent kinase inhibitors; Cytotoxic activity; X-ray structures.
* Corresponding author. Tel.: +420 585634944; fax: +420 585634954; e-mail: trav@risc.upol.cz

0968-0896/$ - see front matter © 2005 Elsevier Ltd. All rights reserved.
doi:10.1016/j.bmc.2005.08.033

protein kinase enzymes which play a crucial role in the regulation of the cell cycle.[20] Some of the first artificially prepared CDK inhibitors based on 6-benzylaminopurine moiety were 2-[2-(hydroxyethyl)amino]-6-benzylamino-9-methylpurine (*Olomoucine*)[21] and 2-[3-(hydroxypropyl)amino]-6-benzylamino-9-isopropylpurine (*Bohemine*) followed by a very effective inhibitor 2-{[l-(hydroxylmethyl)-propyl]-amino}-6-benzylamino-9-isopropylpurine (*Roscovitine*).[22] The above-mentioned organic substances are also very effective against some human cancer cell lines.[22] It was established, that the cytotoxic activity of the molecules with 6-benzylaminopurine moiety, substituted by –OH, $–CH_3$, –Cl, –F or $–OCH_3$ on the phenyl ring, changes after the coordination of the ligand to a suitable transition metal ion, for example, Pt(II), Pd(II),[12] Cu(II),[23] Ni(II)[24,25] or Co(II).[26] These facts brought us into the idea to use four new substituted 6-benzylaminopurine-derived CDK inhibitors as ligands for the preparation and study of Pt(II) and Pd(II) complexes. The compounds used as ligands in this study, that is, 2-{[l-(hydroxylmethyl)-propyl]amino}-6-[(3-hydroxybenzyl)-amino]-9-isopropyl-purine ($\mathbf{L_1}$), 2-{[l-(hydroxymethyl)-2-(methyl)propyl]-amino}-6-[(3-hydroxybenzyl)amino]-9-isopropyl-purine ($\mathbf{L_2}$), 2-chloro-6-[(3-hydroxybenzyl)-amino]-9-isopropyl-purine ($\mathbf{L_3}$) and 2-chloro-6-[(2-hydroxy-3-methoxy)-benzylamino]-9-isopropylpurine) ($\mathbf{L_4}$), are shown in Figure 1.

In this paper, we report the preparation and characterization of a series of *cis*-Pt(II) and *trans*-Pd(II) complexes containing the above-mentioned ligands $\mathbf{L_1}$–$\mathbf{L_4}$. The prepared complexes **1**–**6**, with the composition $[M(L)_2Cl_2]$ {M = Pt(II) or Pd(II)}, have a square-planar geometry with two chloride anions and two organic ligands attached to Pd(II) or Pt(II) central atom via N(7) of the purine ring. In the complexes **1** and **2**, the chloride anions as well as the organic ligands are coordinated to central atom in *cis*-configuration, while in the complexes **3**–**6** in *trans*-geometry.

2. Results and discussion

2.1. Chemistry

The organic ligands were synthesized by slightly modified procedures as described in the literature[22] (Scheme 1).

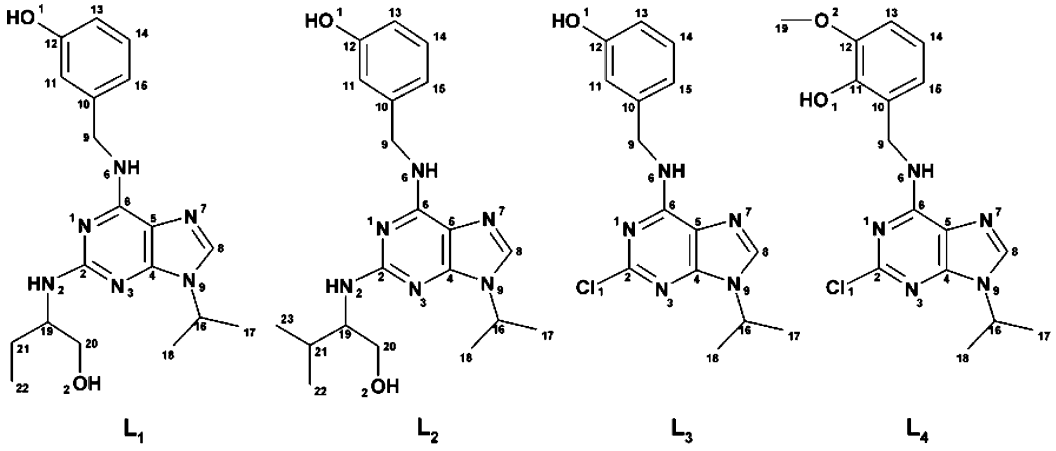

Figure 1. The organic ligands $\mathbf{L_1}$–$\mathbf{L_4}$ used as starting reagents in this study.

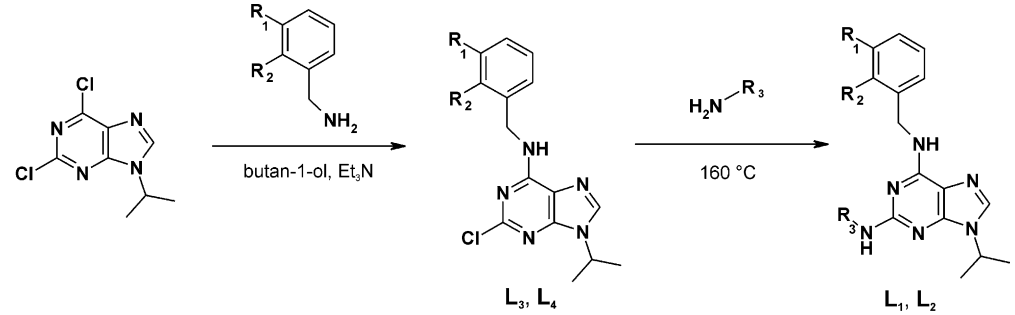

R_1 = -OH (L_1-L_3) R_3 = -(hydroxymethyl)propyl (L_1)
-O-Me (L_4) -(hydroxymethyl)-2-(methyl)propyl (L_2)
R_2 = -H (L_1-L_3)
-OH (L_4)

Scheme 1. Schematic representation of the synthesis of the ligands $\mathbf{L_1}$–$\mathbf{L_4}$.

The mononuclear Pt(II) and Pd(II) complexes described in this paper were prepared by the reaction of *cis*-$[Pt(DMSO)_2Cl_2]$ (Scheme 2), *trans*-$[Pd(DMSO)_2Cl_2]$ or $[K_2PdCL_4]$ (Scheme 3) with the corresponding cyclin-dependent kinase inhibitors $\mathbf{L}_1$–$\mathbf{L}_4$. The syntheses of the complexes were performed in a 1:2 molar ratio of reactants in ethanol and led to the complexes of the types *cis*-$[Pt(L)_2Cl_2]$, where L = $\mathbf{L}_1$ or $\mathbf{L}_2$, and *trans*-$[Pd(L)_2Cl_2]$, where L = $\mathbf{L}_1$–$\mathbf{L}_4$. The molar conductivity values of all the prepared complexes were determined in dimethylformamide (DMF) and acetone solutions, and were found to be 3.7–5.8 and 1.4–17.4 S cm^2 mol^{-1} in DMF, and acetone, respectively. While the molar conductivity value interval for the electrolytes 1:1 is between 65 and 90 S cm^2 mol^{-1} for DMF and between 100 and 140 S cm^2 mol^{-1} for acetone solutions,[27] the obtained conductivity values of the complexes **1**–**6** indicate that the complexes in question behave as non-electrolytes. This finding refers to the fact that both chloride anions and organic ligands are located in the internal coordination sphere of Pt(II) or Pd(II) complexes **1**–**6**.

Despite the fact that the complexes **5** and **6** were supposed to be *cis*-isomers due to the use of $[K_2PdCl_4]$ as a starting complex (in connection with *trans*-effect), it was proved that they are formed in *trans*-arrangement. This finding might be explained by the isomerization of the initial *cis*-complexes after the recrystallization from DMF. A similar behaviour has already been described in the literature for complexes *trans*-$[PtCl_2(L)_2]$ (L = aniline,[9] cyclobutylamine[28] or aminobenzonitrile[29]) and *trans*-$[PdCl_2(L)_2]$, where L = aminobenzonitrile.[29]

2.2. ^{1}H, ^{13}C and ^{195}PtNMR spectroscopy

The chemical shifts in ^{1}H and ^{13}C NMR spectra of the complexes **1**–**6** are listed in Table 1. ^{1}H and ^{13}C NMR spectra are well defined and the signals in the spectra confirm the presence of organic ligands ($\mathbf{L}_1$–$\mathbf{L}_4$) in the complexes **1**–**6**. The ^{1}H NMR spectra of the complexes displayed two important signals assignable to (C8)H and (N6)H. The signals are shifted downfield, $\Delta\delta$ = 0.36–0.77 ppm, where $\Delta\delta = \delta_{complex} - \delta_{ligand}$, towards those belonging to the corresponding atoms in the free CDK inhibitors. The above-mentioned coordination shifts may be connected with probable binding of the transition metal to N7. At this point, we would like to notice that the changes of the chemical shifts of N(6)H may also be caused by the exchange interactions with the protons of the solvent or by the formation of the N–H ⋯ Cl hydrogen bond (see below in Section 2.6.2). Significant shifts were also observed in the ^{13}C NMR spectra. As apparent from Table 1, the largest chemical shifts were found for C5 and C8 of the purine moiety. The signals assigned to C5 are shifted upfield, $|\Delta\delta|$ = 2.95–3.59 ppm, and the signals of C8 downfield, $\Delta\delta$ = 2.84–3.15 ppm, in comparison with the C5 and C8 atom signals in the corresponding free ligands. These carbon atoms are adjacent to N7, that is, the expected coordination site. This conclusion is in agreement with the findings related to the ^{1}H NMR spectra, where the significant coordination chemical shifts for (C8)H and (N6)H were also found.

^{195}Pt-NMR signals of **1** and **2** were observed at −2031 and −2035 ppm as broad ones. These values indicate the existence of the complexes with *cis*-PtN_2Cl_2 chromophores.[30,31] The results are in accord with data published in the literature for *cis*-$[Pt(L)_2Cl_2]$ complexes which vary from −1998 to −2096 ppm (for L = pyridine, lutidine or picoline derivatives, 5,7-disubstituted-1,2,4-triazolo[1,5*a*]pyrimidines).[7,32] The value of −2028 ppm for the *cis*-$[Pt(Boh)_2Cl_2]\cdot 3H_2O$ has also been published.[12]

2.3. IR spectra

The FT-IR spectra of the complexes **1**–**6** were measured in the region 150–4000 cm^{-1} and selected maxima are given in Table 2. Majority of the bands in the region 665–900 cm^{-1} have been assigned to the characteristic skeletal vibrations of the purine ring in the organic ligands. The strong bands, observed between 3359 and 3435 cm^{-1}, could be connected with ν(N–H) and can also be overlapped with those for ν(O–H) of lattice water.[33] The medium bands appearing between 3070 and 3129 cm^{-1} are probably associated with ν(O–H) of a R–CH_2–OH group. Medium absorptions occurring

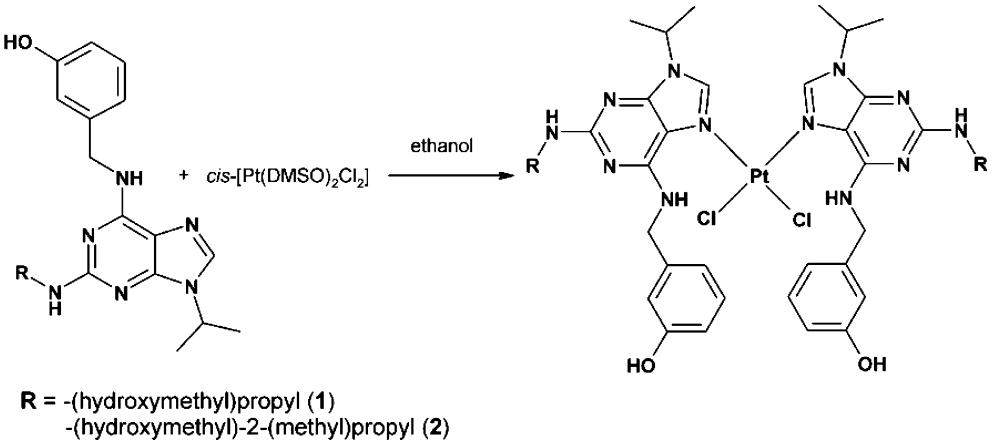

Scheme 2. Schematic representation of the synthesis of *cis*-Pt(II) complexes **1** and **2**.

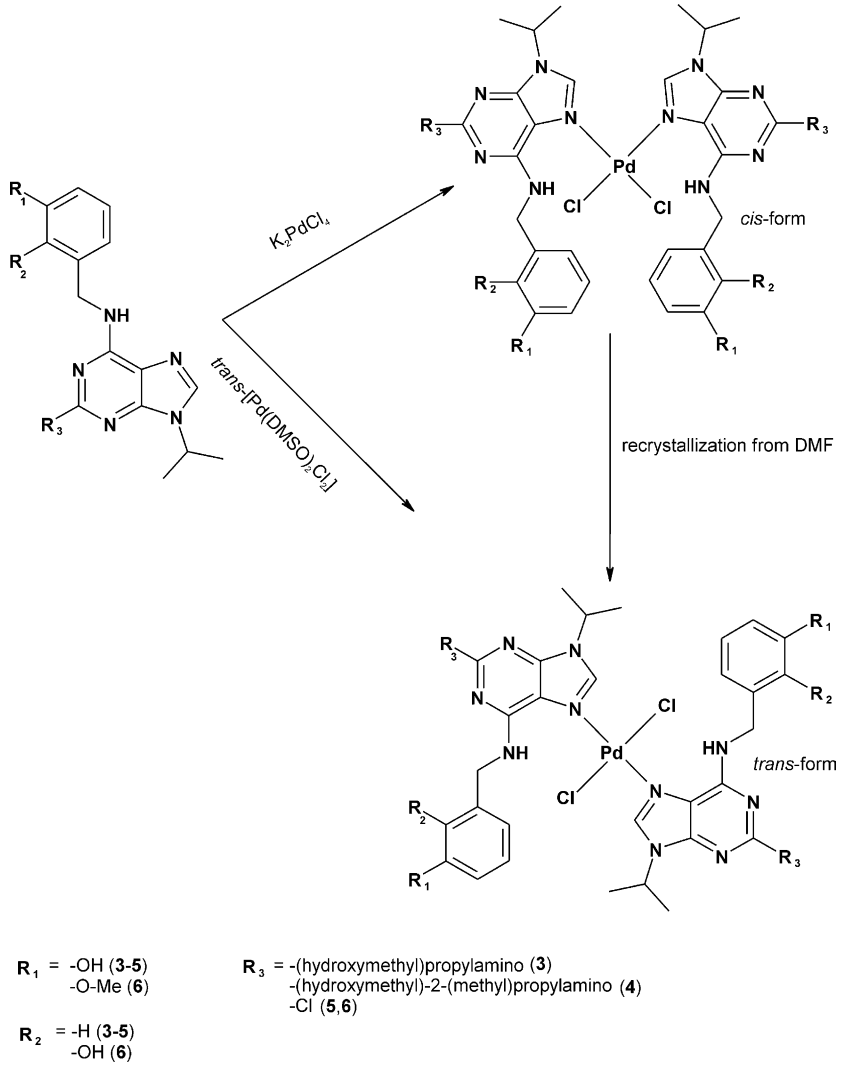

Scheme 3. Schematic representation of the synthesis of *trans*-Pd(II) complexes **3**–**6**.

Table 1. Selected ^{1}H, ^{13}C and ^{195}PtNMR spectral data (δ, ppm) for $\mathbf{L_1}$–$\mathbf{L_4}$ and for the complexes **1**–**6** measured in DMF-d_7

Compounds	(N6)H	(C8)H	C2	C4	C5	C6	C8	^{195}Pt
$\mathbf{L_1}$	7.60	7.77	160.27	151.77	114.90	155.68	135.68	—
$\mathbf{L_2}$	7.58	7.77	160.54	151.77	114.88	155.63	135.65	—
$\mathbf{L_3}$	8.59	8.28	158.71	150.56	119.67	153.97	140.02	—
$\mathbf{L_4}$	8.33	8.29	156.20	150.43	119.71	153.86	140.12	—
1 *cis*-$[Pt(L_1)_2Cl_2]\cdot H_2O$	8.16(0.56)	8.47(0.70)	160.45(0.18)	150.78(−0.99)	111.31(−3.59)	153.60(2.08)	138.57(2.89)	−2031
2 *cis*-$[Pt(L_2)_2Cl_2]\cdot 3H_2O$	8.15(0.57)	8.46(0.69)	160.81(0.27)	150.79(−0.98)	111.33(−3.55)	153.60(−2.03)	138.57(2.92)	−2035
3 *trans*-$[Pd(L_1)_2Cl_2]\cdot H_2O$	8.37(0.77)	8.18(0.41)	160.45(0.18)	151.30(−0.47)	111.85(−3.05)	153.81(−1.87)	138.52(2.84)	—
4 *trans*-$[Pd(L_2)_2Cl_2]\cdot H_2O$	8.17(0.59)	8.36(0.59)	160.76(0.22)	151.28(−0.49)	111.79(−3.09)	153.75(−1.88)	138.78(3.13)	—
5 *trans*-$[Pd(L_3)_2Cl_2]\cdot 2DMF$	8.95(0.36)	8.86(0.58)	158.79(0.08)	150.20(−0.36)	116.72(−2.95)	154.16(0.19)	143.17(3.15)	—
6 *trans*-$[Pd(L_4)_2Cl_2]\cdot 2DMF$	8.99(0.66)	8.84(0.55)	155.16(−1.04)	150.16(−0.27)	116.73(−2.98)	154.22(0.36)	143.07(2.95)	—

Coordination chemical shifts ($\Delta\delta = \delta_{complex} - \delta_{ligand}$) are given in parentheses.

in the 2963–2983 cm^{-1} region could be attributed to the $\nu(C–H)_{ar}$ vibration.[33] A very strong band within the 1610–1616 cm^{-1} region assigned to the $\nu(C{=}N)$ vibration of the purine ring was observed.[33] Medium to strong bands between 1229 and 1267 cm^{-1} can be associated with the $\nu(C–O)_{ar}$ vibration.[33] A strong band observed at 1070 cm^{-1} in the spectra of the complexes could be assigned to the ν(C–O) vibration of the R–CH_2–OH group.[33]

The spectra of the complexes **1**–**6** between 150 and 600 cm^{-1} revealed two new absorption bands, as compared to the spectra of free CDK inhibitors, which could be assigned to ν(M–N) and ν(M–Cl) stretching vibrations. For the platinum(II) complexes **1** and **2**, one split band within the 327–345 cm^{-1} region assignable to the ν(Pt–Cl) stretching vibration was detected. The position as well as the splitting of the band supports our presumption, based mainly on ^{195}Pt NMR spectra, that

Table 2. Selected IR spectral and conductivity data of the complexes **1**–**6**

Compounds	ν(N–H)	ν(O–H)$_{ar}$	ν(C–H)$_{ar}$	ν(C=N)	ν(C$_{ar}$–O)	ν(M–N)	ν(M–Cl)	(S cm^2 mol^{-1})
1 *cis*-[Pt(L$_1$)$_2$Cl$_2$]·H$_2$O	3410s	3070w	2967m	1610vs	1267m	514w 508w	342s 329m	16.5[a] 3.7[b]
2 *cis*-[Pt(L$_2$)$_2$Cl$_2$]·3H$_2$O	3435s	—	2965m	1612s	1266m	531s 510w	345m 327m	16.4[a] 3.8[b]
3 *trans*-[Pd(L$_1$)$_2$Cl$_2$]·H$_2$O	3376s	3118w	2967m	1610vs	1267s	475m	357s	17.0[a] 4.8[b]
4 *trans*-[Pd(L$_2$)$_2$Cl$_2$]·H$_2$O	3427s	3100w	2963m	1610vs	1266m	490m	364m	17.4[a] 6.7[b]
5 *trans*-[Pd(L$_3$)$_2$Cl$_2$]·2DMF	3369s	3129w	2983m	1610vs	1229s	497s	370vs	1.7[a] 5.2[b]
6 *trans*-[Pd(L$_4$)$_2$Cl$_2$]·2DMF	3359s	3100s	2983m	1616vs	1239m	475m	368s	1.4[a] 5.8[b]

[a] Measured in dimethylformamide.
[b] Measured in acetone.

the complexes occur in *cis*-arrangement.[34] The bands in the range of 508–531 cm^{-1} could be assigned to the ν(Pt–N) stretching vibration in the platinum(II) complex with *cis*-configuration.[34] For the palladium(II) complexes **3**–**6**, some single bands between 357 and 370 cm^{-1} which were attributed to the ν(Pd–Cl) vibration were observed,[34] while the bands within the 475–497 cm^{-1} range were assignable to the ν(Pd–N) stretching vibration and are in good agreement with the maximum at 472 cm^{-1}, as found for *trans*-[Pd(L)$_2$Cl$_2$] (L = pyridine) in the literature.[34,35] The maxima at 357–370 cm^{-1} assigned to ν(Pd-Cl) are 10–20 cm^{-1} shifted in comparison to those for *trans*-[Pd(L)$_2$Cl$_2$] complexes, where L = pyridine (358 cm^{-1}) or aniline (334 cm^{-1}) published previously.[35] The single bands observed in these regions supported our belief that the complexes **3**–**6** are in *trans*-arrangement.

2.4. ES+ MS spectroscopy

Electrospray mass spectra in the positive ion mode (ES+ MS) were measured for the complexes **1**–**6**. The molecular ion peaks [M+H]$^+$ were clearly observed at 1007.2, 1035.2, 917.3 and 945.9 *m*/*z*, for **1**, **2**, **3** and **4**, respectively. Peaks were found at 1029.1 *m*/*z* for **1** and 1057.2 *m*/*z* for **2**, related to [M+Na]$^+$, or peaks at 1045.9, 1073.3, 956.2 and 912.0 *m*/*z* for **1**, **2**, **3** and **6**, respectively, related to [M+K]$^+$. The presence of clusters of the molecular ion peaks with Na$^+$ and K$^+$ was caused by the common presence of these ions in the analyzer or in solvent as typical for this type of ionization. Peaks were found at 876.3 *m*/*z* for **4**, 742.9 *m*/*z* for **5** and 803.7*m*/*z* for **6** assignable to [{Pd(L)$_2$}+H]$^+$, and the peak at 971.2 *m*/*z* for **1** attributable to [{Pd(L)$_2$Cl}+H]$^+$. In all the complexes **1**–**6**, [L+H]$^+$ peaks of the corresponding CDK inhibitors were found, that is, at 371.0 *m*/*z* for **1** and **3**, 385.2 *m*/*z* for **2** and **4**, 318.1 *m*/*z* for **5** and 348.1 *m*/*z* for **6**. In all the complexes, except for **2**, the peaks for [L+Na]$^+$ were observed. In the spectra of the complex **6**, the peak at 386.0 *m*/*z* for [L+K]$^+$ was also detected. In all the complexes, the fragmentation of the organic ligand was observed. The peaks with the values ca. 121 *m*/*z*, found for **2**–**6**, can be assigned to [purine+H]$^+$, whilst the peaks at ca. 137 *m*/*z*, found for **1**, **3** and **4** complexes, can be ascribed to [adenine+H]$^+$. The peak at 163.0 *m*/*z* appeared in the spectra of complex **4** which can be associated with [9-isopropylpurine+H]$^+$. Unfortunately, we did not obtain any peaks which represent the more extensive fragmentation of the ligands, because massive recombination of the fragments occurs when using the used voltages.

2.5. Thermal analyses

Thermogravimetric analysis (TGA) and differential scanning calorimetry (DSC) were used for the thermal behaviour study of the complexes **1**–**6**. The thermal decompositions of Pt(II) *cis*-complexes **1** and **2** started between 60 and 90 °C and ended at ca 580 °C. In the above-mentioned temperature interval, there appeared to be some weight losses, accompanied by broad *endo*-effects on DSC curves with the minimum at 78.1 °C for **1** and 66.7 °C for **2**, corresponding to the elimination of one crystal water molecule for **1** (found/calcd: 1.7/1.8%), or three crystal water molecules for **2** (found/calcd: 5.6/5.8%). For the complexes **1** and **2**, the activation energy of the above-mentioned *endo*-effects was determined by the Borchardt and Daniels method,[36] and was found to be 28.8 kJ mol^{-1} (6.9 kcal mol^{-1}) for **1** or 40.3 kJ mol^{-1} (9.6 kcal mol^{-1}) for **2**. Between 360 and 500 °C, weight losses were observed accompanied by appropriate *exo*-effects on DSC curves. These weight losses were not associated with the formation of the thermally stable intermediates. However, there occurred some significant slowing in weight loss on TG curves around 380 °C, which might be connected with the loss of one molecule of organic ligand (found/calcd: 35.7/35.9%) and (found/calcd: 35.6/35.8%), for the complexes **1**, and **2**, respectively.

The thermal decomposition of the *trans*-Pd(II) complexes **3**–**6** is similar and started within the temperature interval 80–120 °C. Clearly observable weight losses on TG curves, which appeared between 50 and 120 °C, were accompanied with the *endo*-effects on DSC curves and assigned to the elimination of one crystal water molecule for **4** (found/calcd: 1.7/1.8%), two molecules of DMF for **5** (found/calcd: 17.2/16.9%) and for **6** (found/calcd: 14.2/14.3%). The minima of the *endo*-effects were found to be 55.6, 132.7, 112.2 °C for **4**, **5** and **6**, respectively. In the case of **3**, a weight loss relating to crystal water elimination could not be assigned

due to overlapping with another decomposition process. The DSC and TG curves of the complex **6** are presented in Figure 2. In the complex **6**, a significant weight loss was observed between 260 and 290 °C accompanied by the sharp *endo*-effect with the minimum at 269.0 °C, which is probably connected with the loss of one molecule of organic ligand from the complex **6** (found/calcd: 34.0/34.1%). Then, the thermal decomposition of **6** proceeds without the formation of stable intermediates and is finished at ca. 570 °C. For **4**–**6**, the activation energy of the endothermic effect assignable to the crystal H_2O (**4**) or DMF (**5**,**6**) elimination was also determined[36] and was found to be 28.8 (6.9), 254.3 (60.7) and 259.6 (62.0) kJ mol^{-1} (kcal mol^{-1}) for **3**, **4**, **5** and **6**, respectively.

2.6. X-ray crystallography

2.6.1. X-ray structure of 2-{[l-(hydroxymethyl)propyl]-amino}-6-[(3-hydroxybenzyl)amino]-9-isopropyl-purine, (L_1).

The molecular structure of $\mathbf{L}_1$ together with the atom numbering scheme is shown in Figure 3. The crystallographic data are given in Table 3, while selected bond lengths and angles can be found in Table 4. The intermolecular parameters of the adenine moiety of $\mathbf{L}_1$ are in good agreement with those found for the similar compounds described previously, for example, 6-(2-chlorobenzyl-amino)purine (L_a)[37] or 6-benzylaminopurine (L_b).[38] For example, the C(2)–N(3)–C(4) angle which is 111.6(3)° for $\mathbf{L}_1$ is 111.32(14)° for L_a and 110.70° for L_b.[37,38] From a general point of view, we can state that the protonation and/or substitution of the ligand cause the differences in the interatomic parameters within the purine ring, mainly in C–N–C bond angles. For example, the value of 111.6(3)° for the C(2)–N(3)–C(4) bond angle in $\mathbf{L}_1$ differs significantly in comparison with those for the N3 protonated forms of similar molecules. The values for the above-mentioned angle were found to be 117.02(16)° in 6-(4-methoxybenzylamino)purin-3-ium chloride, (H^+L_d),[39] and 117.6(2)° in 6-(3-chlorobenzylamino)purin-3-ium chloride, (H^+L_e).[37]

Other differences in bond angles between the electroneutral and protonated forms of these molecules are observable also for the C(8)–N(7)–C(5) and C(8)–N(9)–C(4) angles, mainly in cases where the molecules are protonated or substituted at N7 and/or N9 positions. Concretely, the values of 104.6(3)° and 105.6(3)° for the angles C(8)–N(7)–C(5) and C(8)–N(9)–C(4), respectively, of $\mathbf{L}_1$ differ significantly from those found for H^+L_e {106.8(2)° and 102.60(18)°}[37] and H^+L_f {108.10(19)° and 108.05(19)°},[40] where H^+L_f is 6-benzylamino-2-(2-hydroxyethylamino)-9-methylpurine-1,7-diium bis(perchlorate) monohydrate. The changes relating to different degree of protonation and/or substitution within the 6-benzylaminopurine moieties are also apparent for select-

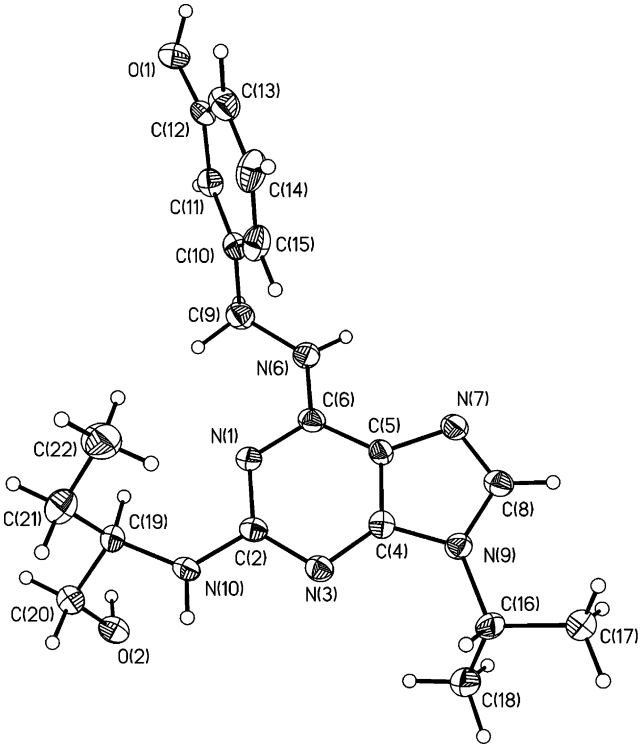

Figure 3. The molecular structure of $\mathbf{L}_1$ together with the atom numbering scheme. The thermal ellipsoids are plotted at the 50% probability level.

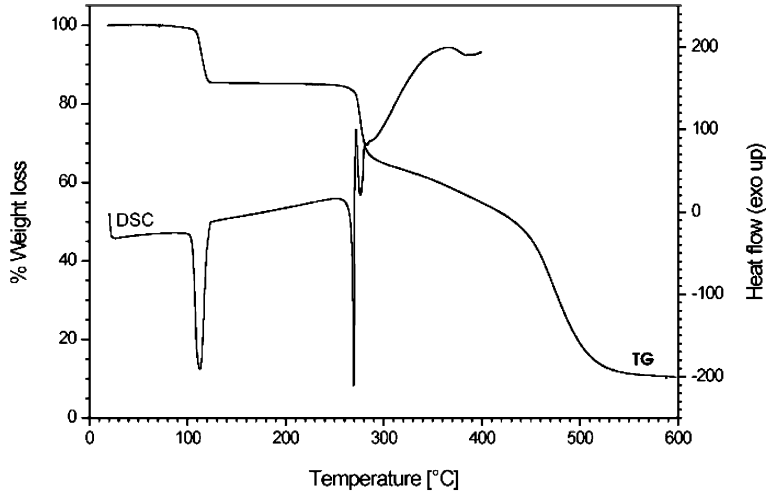

Figure 2. DSC and TG curves of the complex **6**.

Table 3. Crystal data and structure refinements for $\mathbf{L_1}$, *trans*-$[Pd(L_3)_2Cl_2]\cdot 2DMF$ (**5**) and *trans*-$[Pd(L_4)_2Cl_2]\cdot 2DMF$ (**6**)

Compound	$\mathbf{L_1}$	**5**	**6**
Empirical formula	$C_{19}H_{26}N_6O_2$	$C_{36}H_{46}Cl_4N_{12}O_4Pd$	$C_{38}H_{50}Cl_4N_{12}O_6Pd$
Molecular weight	370.46	959.05	1019.11
Temperature (K)	100(2)	100(2)	100(2)
Crystal system	Monoclinic	Monoclinic	Triclinic
Space group	$P2_1$	$P2_1/n$	$P-1$
Unit cell dimensions			
a (Å)	9.579(2)	9.3882(6)	9.4982(6)
b (Å)	5.8454(12)	19.9915(13)	10.9058(8)
c (Å)	17.241(3)	10.9270(7)	11.8499(8)
α(°)	90.0	90.0	80.390(6)
β(°)	93.52(2)	96.437(6)	78.262(6)
γ(°)	90.0	90.0	66.535(7)
V(Å^3)	963.6(3)	2037.9(2)	1097.37(13)
Z	2	2	2
Density (g cm^3)	1.277	1.563	1.542
μ (mm^{-1})	0.087	0.773	0.726
F(000)	396	984	524
Crystal size (mm)	$0.20\times0.15\times0.15$	$0.40\times0.40\times0.35$	$0.25\times0.25\times0.20$
Index ranges (h, k, l)	$-11\leqslant h\leqslant 11$ $-6\leqslant k\leqslant 6$ $-20\leqslant l\leqslant 20$	$-11\leqslant h\leqslant 10$ $-21\leqslant k\leqslant 23$ $-12\leqslant l\leqslant 12$	$-9\leqslant h\leqslant 11$ $-12\leqslant k\leqslant 12$ $-13\leqslant l\leqslant 14$
Reflections collected/unique	5488/1865	12496/3550	8339/3849
Data /restraints/parameters	1865/1/252	3550/0/263	3849/0/282
Goodness-of-fit on F^2	0.978	1.127	1.094
Final R_1/wR_2 indices [$I > 2\sigma(I)$]	0.0505/0.1199	0.0370/0.0882	0.0313/0.0720
R_1/wR_2 indices (all data)	0.0601/0.1260	0.0384/0.0878	0.0354/0.0737

ed dihedral and torsion angles. In $\mathbf{L_1}$, the torsion angles for C(6)–N(6)–C(9)–C(10), C(5)–C(6)–N(6)–C(9) and N(6)–C(9)–C(10)–C(15) are 106.5(4)°, −168.4(4)° and −41.7 (5)°, respectively. For comparison, these torsion angles for an N3-protonated N7 tautomers, for example, H^+L_e, are −129.5(2)°, 178.99(17)° and 49.7(3)°, respectively,[37] and as can be seen they differ significantly as against those found for an electroneutral form of the $\mathbf{L_1}$ molecule. The $\mathbf{L_1}$ molecule contains nearly planar benzene (*A*), pyrimidine (*B*) and imidazole (*C*) ring systems with maximal deviations from each plane of 0.0114(26), 0.0037(25) and 0.0090(22) Å for rings *A*, *B* and *C*, respectively. Atoms forming the purine ring (*B* + *C*) also deviate significantly from planarity with maximal deviations being 0.0114(25) Å for N(9) atom.[41] The dihedral angle of $\mathbf{L_1}$ between the benzene and the purine rings is 79.01(10)°. This value is in accord with the one published for a similar electroneutral molecule L_a which is 79.5(2)°[37] but differs from the value for protonated H^+L_f being 82(1)°.[40] The *Cg*A…*Cg*B, *Cg*A…*Cg*C and *Cg*B…*Cg*C distances are 5.7196(13), 6.5001(12) and 2.0936(3) Å, respectively, where *Cg*A, *Cg*B and *Cg*C are the centroids of the rings *A*, *B* and *C*, respectively. The crystal structure of $\mathbf{L_1}$ is stabilized by a network of N–H···O and O–H···N hydrogen bonds. More detailed information related to hydrogen bonding of $\mathbf{L_1}$, including symmetry transformations, is given in Table 5.

2.6.2. X-ray structures of *trans*-$[Pd(L_3)_2Cl_2]\cdot 2DMF$ (5) and *trans*-$[Pd(L_4)_2Cl_2]\cdot 2DMF$ (6). The molecular structures of the complexes **5** and **6** have also been determined and they are depicted in Figures 4 and 5, respectively.

The crystallographic data are given in Table 3, while selected bond lengths and angles can be found in Table 4. The orange crystals of the complexes **5** and **6** have been prepared by recrystallization of the compounds from DMF. Both the complexes (**5**, **6**) have a square-planar arrangement of donor atoms in the vicinity of palladium with a PdN_2Cl_2 chromophore. In both cases, two chlorine atoms and two organic ligands, bonded via N(7) atom of the imidazole ring, are coordinated to the palladium atom in a *trans*-geometry. Atoms forming the benzene and purine ring deviate slightly from planarity in both the complexes **5** and **6**.

The maximal deviations from the above-mentioned rings in the complex **5** are 0.0026(21) Å for C(11) and 0.0493(24) Å for C(5), while 0.0113(23) Å for C(4) and 0.0107(19) Å for C(11) in the complex **6**.[41] The *Cg*A…*Cg*B, *Cg*A…*Cg*C and *Cg*B…*Cg*C distances were found to be 5.5277(3), 6.8413(3) and 2.0882(1) Å, respectively, in the complex **5**, while the same distances are equal to 5.5227(6), 6.7747(7) and 2.0899(1) Å, respectively, in the complex **6**. To date, only one similar structure having the *trans*-PdN_2Cl_2 chromophore and purine moiety at the molecule has been deposited with the Cambridge Crystallographic Centre CCDC (CSD Version 5.25.),[42] that is, *trans*-dichloro-bis(inosine)-palladium(II) pentahydrate, *trans*-$[Pd(Ino)_2Cl_2]\cdot 5H_2O$, where each of the purine rings of two inosine ligands is bonded via N(7) atom to palladium in *trans*-arrangement.[14] The Pd(l)–N(7) bond length is 2.019(2) Å (for **5**) and 2.010(2) Å (for **6**), which is within an interval 1.991–2.018 Å of the values published for the above-mentioned structure.[14]

Table 4. Selected bond lengths (Å) and angles (°) for $\mathbf{L}_1$, *trans*-$[Pd(L_3)_2Cl_2]\cdot 2DMF$ (**5**) and *trans*-$[Pd(L_4)_2Cl_2]\cdot 2DMF$ (**6**)

	$\mathbf{L}_1$	**5**	**6**
Bond lengths			
Pd(l)–N(7)	—	2.019(2)	2.010(2)
Pd(l)–N(7A)	—	2.019(2)	2.010(2)
Pd(l)–Cl(l)	—	2.2809(7)	2.3014(7)
Pd(l)–C1(1A)	—	2.2809(7)	2.3014(7)
N(l)–C(2)	1.353(4)	1.333(4)	1.328(4)
N(l)–C(6)	1.343(5)	1.354(4)	1.355(3)
N(3)–C(2)	1.365(5)	1.313(4)	1.317(4)
N(3)–C(4)	1.343(5)	1.350(4)	1.350(3)
N(7)–C(8)	1.315(5)	1.320(4)	1.322(3)
N(7)–C(5)	1.400(6)	1.391(4)	1.396(3)
N(9)–C(8)	1.374(4)	1.354(4)	1.353(3)
N(9)–C(4)	1.375(5)	1.374(4)	1.374(3)
C(4)–C(5)	1.378(5)	1.386(4)	1.382(4)
C(5)–C(6)	1.400(6)	1.415(4)	1.414(4)
Bond angles			
N(7)–Pd(l)–N(7A)	—	180.0	180.0
N(7A)–Pd(l)–Cl(l)	—	91.18(7)	91.81(6)
N(7)–Pd(l)–C1(1A)	—	91.18(7)	91.81(6)
N(7)–Pd(l)–Cl(l)	—	88.82(7)	88.19(6)
N(7A)–Pd(l)–Cl(lA)	—	88.82(7)	88.19(6)
Cl(l)–Pd(l)–Cl(lA)	—	180.0	180.0
C(8)–N(7)–Pd(l)	—	122.83(19)	123.02(18)
C(5)–N(7)–Pd(l)	—	130.79(19)	130.83(17)
C(2)–N(1)–C(6)	118.7(3)	117.7(2)	117.7(2)
C(2)–N(3)–C(4)	111.6(3)	109.9(2)	109.5(2)
C(8)–N(7)–C(5)	104.6(3)	106.0(2)	106.0(2)
C(8)–N(9)–C(4)	105.6(3)	106.7(2)	107.0(2)
N(3)–C(2)–N(1)	127.2(3)	131.2(3)	131.5(2)
N(3)–C(4)–N(9)	126.7(3)	126.2(3)	126.2(2)
N(3)–C(4)–C(5)	126.2(4)	127.0(3)	127.0(2)
N(9)–C(4)–C(5)	107.1(3)	106.8(2)	106.8(2)
C(4)–C(5)–N(7)	109.4(3)	108.3(2)	108.2(2)
C(4)–C(5)–C(6)	117.5(3)	116.5(3)	116.9(2)
N(7)–C(5)–C(6)	133.1(3)	134.9(3)	134.9(2)
N(1)–C(6)–C(5)	118.7(3)	117.7(3)	117.4(2)
N(7)–C(8)–N(9)	113.4(4)	112.2(2)	111.9(2)

Symmetry transformations used to generate equivalent atoms A: for **5**: $-x$, $-y+2$, $-z+1$; for **6**:$-x+2$, $-y$, $-z+2$.

Table 5. Hydrogen-bonding geometry for ligand $\mathbf{L}_1$, *trans*-$[Pd(L_3)_2Cl_2]\cdot 2DMF$ (**5**) and *trans*-$[Pd(L_4)_2Cl_2]\cdot 2DMF$ (**6**) [Å, °]

D–H···A	d(D–H)	d(H···A)	d(D···A)	<(DHA)
For $\mathbf{L}_1$				
N(10)–H(10A)–O(2)^{i}	0.88	2.12	2.936(4)	154.8
O(l)–H(l)–N(7)^{ii}	0.85(6)	1.89(6)	2.656(4)	149(6)
O(2)–H(2)–N(3)^{iii}	0.93(6)	1.87(6)	2.789(4)	168(5)
N(6)–H(6A)–O(l)^{iv}	0.88	2.06	2.889(4)	155.9
For **5**				
N(6)–H(6A)···C1(1)^{v}	0.88	2.82	3.382(3)	122.7
O(1)–H(1A)···O(2)^{v}	0.84	1.81	2.625(3)	162.5
For **6**				
O(1)–H(1)···O(2)^{vi}	0.84	2.21	2.661(3)	113.8
O(l)–H(l)···Cl(l)^{vii}	0.84	2.45	3.216(2)	151.2
N(6)–H(6A)···O(3)^{vi}	0.88	2.62	3.161(3)	120.4

Symmetry transformations used to generate equivalent atoms: (i): $-x+1$, $y+1/2$, $-z+1$; (ii): $-x$, $y-1/2$, $-z$; (iii): x, $y-1$, z; (iv): $-x$, $y+1/2$, $-z$; (v): $-x$, $-y+2$, $-z+1$; (vi): $-x+2$, $-y$, $-z+2$; (vii): $x-1$, y, z.

The Pd–Cl distances are 2.2809(7) Å for **5** and 2.3014(7) Å for **6**, and differ significantly from those reported previously for *trans*-$[Pd(Ino)_2Cl_2]\cdot 5H_2O$ {2.296(2) and 2.343(2) Å}[14] and $[PdCl(L)]^+$ (L = chelate-tethered derivatives of adenine)[43] {2.3189(9) and 2.300(10) Å}. A degree of deformation in a square-planar arrangement in the vicinity of the central atom can also be deduced from angle values because they vary significantly from the idealized 90°. The N(7)–Pd(l)–C1(1A) angle equals 91.18(7)° (for **5**) and

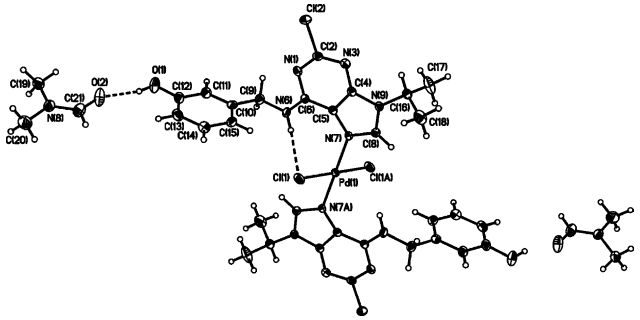

Figure 4. The molecular structure of **5** including the atom numbering scheme. The thermal ellipsoids are plotted at the 50% probability level. Hydrogen bonds are shown as dashed lines.

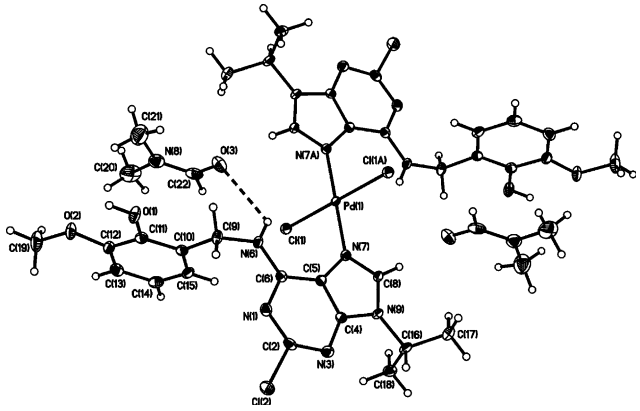

Figure 5. The molecular structure of **6** including the atom numbering scheme. The thermal ellipsoids are plotted at the 50% probability level. Hydrogen bonds are shown as dashed lines.

91.81(6)° (for **6**), whilst the value determined for the N(7)–Pd(l)–Cl(l) angle is 88.82(7)° (for **5**) and 88.19(6)° (for **6**). The bond angle values around the central atom slightly differ from those described in the structure for *trans*-$[Pd(Ino)_2Cl_2]\cdot 5H_2O$, where the value for the same angle is 90.4(2)° and 89.0(2)°, respectively.[14]

Spatial arrangement of the organic molecules in **5** and **6** can be deduced from values of selected dihedral and torsion angles. The dihedral angles between the atoms forming the benzene and purine rings are 88.01(8)° and 85.78(6)° for **5** and **6**, respectively.[14] The torsion C(6)–N(6)–C(9)–C(10), C(5)–C(6)–N(6)–C(9) and N(6)–C(9)–C(10)–C(15) angles are −90.4(3)°, −173.3(3)°, −1.1(4)° (for **5**), and −92.9(3), −176.1(2) and 14.4(4)° (for **6**), respectively. The crystal structures of **5** and **6** are stabilized by networks of hydrogen bonds. Hydrogen bonding geometry for both the structures, involving O–H···O, O–H···C1, N–H···Cl and N–H–O hydrogen bonds, is given in Table 5.

2.7. In vitro cytotoxicity studies

The prepared complexes **1**–**6** and the corresponding CDK inhibitors, used as ligands, were tested in vitro against four human cancer cell lines: K-562, MCF7, G-361 and HOS. The IC_{50} cytotoxicity values of the complexes were compared to those found for the starting organic bases as well as for some of the anticancer agents used nowadays, that is, *Cisplatin* and *Oxaliplatin*. The obtained results are presented in Table 6. The IC_{50} values of Pt(II) complexes presented in this work are comparable to those achieved for the starting ligands in case of the MCF7 and K-562 cancer cell lines. However, very interesting results were obtained against G-361 (6 μM) and HOS (6 μM) cell lines for complex **1**. Moreover, the IC_{50} value in the case of the G-361 cell line is approximately five times more effective in comparison to the free CDK inhibitor. The above-mentioned IC_{50} values of the complex **1** are also comparable with those obtained for *Cisplatin*, which are 3 μM against G-361 and 3 μM against HOS, and even better than the results obtained for *Oxaliplatin*, which are 7 μM and 7 μM, against G-361 and HOS, respectively.

Although the free CDK inhibitors $\mathbf{L_3}$ and $\mathbf{L_4}$ are not very effective as is obvious from Table 6 their complexes **5** and **6** demonstrate at least twice higher cytotoxicity against both the lines MCF7 and K-562. Moreover, the cytotoxicity of the complexes **3** and **4** against the

Table 6. Cytotoxicity of the complexes **1**–**6** compared to those found for the organic ligands, *Cisplatin* and *Oxaliplatin*, expressed as IC_{50} values (μM)

Compounds	IC_{50}			
	MCF7	K-562	G-361	HOS
$\mathbf{L_1}$	7	21	29	10
$\mathbf{L_2}$	15	16	7	9
$\mathbf{L_3}$	45	> 50	38	> 50
$\mathbf{L_4}$	> 50	20	31	26
1 *cis*-$[Pt(L_1)_2Cl_2]\cdot H_2O$	15	17	6	6
2 *cis*-$[Pt(L_2)_2Cl_2]\cdot 3H_2O$	19	17	18	21
3 *trans*-$[Pd(L_1)_2Cl_2]\cdot H_2O$	3	7	20	12
4 *trans*-$[Pd(L_2)_2Cl_2]\cdot H_2O$	3	6	15	15
5 *trans*-$[Pd(L_3)_2Cl_2]\cdot 2DMF$	27	29	28	32
6 *trans*-$[Pd(L_4)_2Cl_2]\cdot 2DMF$	29	34	>50	32
Cisplatin	11	5	3	3
Oxaliplatin	18	9	7	7

IC_{50} (μM) specified by a calcein AM assay of surviving tumor cells. The human cancer cell lines[a] were treated with the solution of the tested compound in the concentration range of 0.2–50 μM for 72 h at 37 °C. 5% CO_2. [a]MCF7, breast adenocarcinoma; K-562, chronic myelogenous leukaemia; G-361, malignant melanoma; HOS, osteogenic sarcoma. The figures in the table present the arithmetic mean of three measured values. The measurement deviation ranges from 13 to 19%.

latter cell lines is significantly higher as compared to those determined for *Oxaliplatin* and *Cisplatin*.

3. Experimental

3.1. Materials

K_2PdCl_4 was used as purchased (Sigma-Aldrich Co.), *cis*-[Pt(DMSO)$_2$Cl$_2$] and *trans*-[Pd(DMSO)$_2$Cl$_2$] were prepared according to the published methods.[44,45] The organic ligands 2-{[l-(hydroxymethyl)propyl]amino}-6-[(3-hydroxybenzyl)amino]-9-isopropylpurine (**L**$_1$), 2-{[l-(hydroxymethyl)-2-(methyl)propyl]amino}-6-[(3-hydroxybenzyl)amino]-9-isopropylpurine (**L**$_2$), 2-chloro-6-[(3-hydroxybenzyl)amino]-9-isopropylpurine (**L**$_3$) and 2-chloro-6-[(2-hydroxy-3-methoxybenzyl)amino]-9-isopropylpurine (**L**$_4$) were prepared by the slightly modified methods described in the literature.[22]

The yellowish crystals of **L**$_1$ suitable for single crystal X-ray analysis were obtained by recrystallization from *iso*-propanol. **L**$_1$: found: C, 61.3; H, 7.4; N, 22.6%. $C_{19}H_{26}N_6O_2$ requires C, 61.6;H, 7.1; N, 22.7%, mp: 151–152 °C; TLC: single spot. ^{1}H NMR (DMF-d_7, ppm):9.38 (s, 1H, (O1)H), 7.77 (s, 1H, (C8)H), 7.60 (s, 1H, (N6)H), 7.12 (t, 1H, (C14)H, J = 7.7 Hz), 6.94 (s, 1H, (C11)H), 6.87 (d, 1H, (C15)H, J = 7.5 Hz), 6.71 (dd, 1H, (C13)H, J_a = 7.9 Hz, J_b = 2.2 Hz), 5.82 (d, 1H, (N2)H, J = 7.7 Hz), 4.91 (s, 1H, (02)H), 4.74 (s, 2H, (C9)H), 4.62 (sep, 1H, (C19)H, J = 6.8 Hz), 3.98 (m, 1H, (C16)H), 3.66 (m, 1H$_a$, (C20)H), 3.58 (m, 1H$_b$, (C20)H), 1.74 (sep, 1H$_a$, (C21)H, J = 7.0 Hz), 1.59 (sep, 1H$_b$(C21)H, J = 7.0 Hz), 1.53 (d, 6H, (C17,18)H, J = 6.6 Hz), 0.94 (t, 3H, (C22)H, J = 7.5 Hz). ^{13}C NMR (DMF-d_7, ppm): 160.27 (C2), 158.55 (C12), 155.68 (C6), 151.77 (C4), 143.15 (C10), 135.68 (C8), 129.69 (C11), 118.77 (C15), 115.05 (C14), 114.90 (C5), 114.18 (C13), 64.52 (C20), 55.29 (C19), 46.81 (C16), 43.77 (C9), 24.91 (C21), 22.34 (C17,18), 10.99 (C22). **L**$_2$: found: C, 62.3; H, 7.3; N, 21.9%. $C_{20}H_{28}N_6O_2$ requires C, 62.5; H, 7.3; N, 21.9%, mp: 179–180 °C; TLC: single spot. ^{1}H NMR (DMF-d_7, ppm): 9.43 (s, 1H, (O1)H), 7.77 (s, 1H, (C8)H), 7.58 (s, 1H, (N6)H), 7.12 (t, 1H,(C14)H, J = 7.7 Hz), 6.94 (t, 1H,(C11)H, J = 1.8 Hz), 6.87 (d, 1H,(C15)H, J = 7.5 Hz), 6.71 (dd, 1H, (C13)H, J_a = 7.9 Hz, J_b = 2.2 Hz), 5.82 (d, 1H, (N2)H, J = 7.8 Hz), 4.89 (s, 1H, (O2)H), 4.74 (s, 2H, (C9)H), 4.62 (sep, 1H, (C19)H, J = 6.8 Hz), 3.98 (m, 1H, (C16)H), 3.66 (qui, 2H, (C20)H, J = 4.5 Hz), 2.07 (sxt, 1H, (C21)H, J = 6.8 Hz), 1.53 (dd, 6H, (C17,18)H, J_a = 6.8 Hz, J_b = 1.9 Hz), 0.97 (d, 3H, (C22)H, J = 6.8 Hz), 0.95 (d, 3H, (C23)H, J = 6.8 Hz). ^{13}C NMR (DMF-d_7, ppm): 160.54 (C2), 158.55 (C12), 155.63 (C6), 151.77 (C4), 143.13 (C10), 135.65 (C8), 129.67 (C11), 118.75 (C15), 115.03 (C14), 114.88 (C5), 114.77 (C13), 62.93 (C20), 58.71 (C19), 46.79 (C16), 43.79 (C9), 29.02 (C21), 22.38 (C17), 22.29 (C18), 19.93 (C22), 18.92 (C23). **L**$_3$: found: C, 56.5; H, 5.0; N, 21.6%. $C_{15}H_{16}N_5OC1$ requires C, 56.7; H 5.1; N, 22.0%, mp: 217–218 °C; TLC: single spot. ^{1}H NMR (DMF-d_7, ppm): 9.48 (s, 1H, (O1)H), 8.59 (t, 1H, (N6)H, J = 6.2 Hz), 8.28 (s, 1H, (C8)H),7.14 (t, 1H, (C14)H, J = 7.9 Hz), 6.94 (t, 1H, (C11)H, J = 1.8 Hz), 6.87 (d, 1H, (C15)H, J = 7.5 Hz), 6.73 (dd, 1H, (C13)H, J_a = 7.9 Hz, J_b = 2.3 Hz), 4.76 (sep, 1H, (C16)H, J = 6.8 Hz), 4.75 (d, 2H, (C9)H, J = 6.2 Hz), 1.58 (d, 6H, (C17,18)H, J = 6.8 Hz). ^{13}C NMR (DMF-d_7, ppm): 158.71 (C2), 156.13 (C12), 153.97 (C6), 150.56 (C4), 141.87 (C10), 140.02 (C8), 129.91 (C11), 119.67 (C5), 118.76 (C15), 115.04 (C14), 114.53 (C13), 47.89 (C16), 44.08 (C9), 22.41 (C17,18). **L**$_4$: found: C, 55.2; H, 5.2; N, 19.8%. $C_{16}H_{18}N_5O_2C1$ requires C, 55.2; H 5.2; N, 20.1%, mp: 161 - 162 °C; TLC: single spot. ^{1}H NMR (DMF-d_7, ppm): 9.07 (s, 1H, (O1)H), 8.33 (t, 1H, (N6)H, J = 6.2 Hz), 8.29 (s, 1H, (C8)H), 6.89 (dd, 2H, (C13,15)H, J_a = 7.7 Hz, J_b = 1.8 Hz), 6.74 (t, 1H(C14)H, J = 7.9 Hz), 4.80 (d, 2H, (C9)H, J = 6.2 Hz), 4.78 (sep, 1H, (C16)H, J = 6.8 Hz), 3.84 (s, 3H, (C19)H), 1.58 (d, 6H, (C17,18)H, J = 6.8 Hz). ^{13}C NMR (DMF-d_7, ppm): 156.20 (C2), 153.86 (C6), 150.43 (C4), 148.54 (C12), 145.22 (C11), 140.12 (C8), 126.34 (C10), 121.02 (C15), 119.71 (C5), 119.41 (C14), 111.41 (C13), 56.36 (C19), 47.95 (C16), 39.88 (C9), 22.42 (C17,18).

3.2. Methods

3.2.1. General techniques. Elemental analyses (C, H, and N) were determined on an EA1112 Flash analyzer (ThermoFinnigan). Thin layer chromatography (TLC) was performed using $CHC1_3$/CH_3OH/NH_4OH (8:2:0.1) mobile phase and carried out using silica gel 60 WF_{254} plates (Merck Co.). Melting points (mp) were determined with a BÜCHI Melting Point B-540. Conductivity measurements were performed on a Cond340i/SET conductometer (WTW, Germany) in dimethylformamide (DMF) and acetone solutions (10^{-3} M) at 25 °C. FT-IR spectra in the range 150–600 cm^{-1} were measured using polyethylene (PE) discs or nujo1 technique, while FT-IR spectra in the region 400–4000 cm^{-1} were obtained by the KBr disc technique, both using a NEXUS 670 FT-IR spectrometer (Thermo Nicolet). Thermogravimetric analysis and differential scanning calorimetry (DSC) measurements were performed on a TGA XP-10 Thermogravimetric Analyser (THASS, GmbH). TGA was performed in the range 20–600 °C with the gradient 5 °C per minute, while DSC recorded in the range 20–400 °C with the gradient 5 °C per minute. The measurements were taken in the air atmosphere. ES+ MS spectra were recorded using an electrospray probe on a Waters ZMD 2000 mass spectrometer. The mass monitoring interval was 10–1500 *m*/*z*. All interpretations of *m*/*z* were related to ^{35}C1, ^{194}Pt and ^{104}Pd. The spectra were collected using 3.0 s cyclical scans and applying the sample cone voltage: 20, 40 and 60 V at the source block temperature of 80 °C. Desolvation temperature was 150 °C and desolvation gas flowrate 200 L/h. The mass spectrometer was directly coupled to a Mass Lynx data system.

^{1}H, ^{13}C and ^{195}Pt NMR spectra were recorded on a Bruker Avance 300 spectrometer at 300 K. The sam-

ples were prepared by dissolving of the ligands $\mathbf{L}_1$–$\mathbf{L}_4$ and the complexes **1**–**7** in deuterated dimethylformamide (DMF-d_7). The internal reference standard used for ^{1}H and ^{13}C was tetramethylsilane (TMS), the external standard used for ^{195}Pt was K_2PtCl_6 (δ = 0.0 ppm).

3.2.2. X-ray crystallography. X-ray data of L_1 *trans*-$[Pd(L_3)_2Cl_2]\cdot 2DMF$ (**5**) and *trans*-$[Pd(L_4)_2Cl_2]\cdot 2DMF$ (**6**) were collected on a four-circle κ-axis diffractometer Xcalibur2 (Oxford Diffraction Ltd.) equipped with the Sapphire2 CCD detector at 100 K. The CrysAlis (ver.1.171.23) software was used for data collection and reduction.[46] The structures were solved using the direct methods [SHELXS-97][47] and refined anisotropically on F^2 using full-matrix least-squares procedure [SHELXL-97].[41] All hydrogen atoms of $\mathbf{L}_1$, **5** and **6** were localized in difference Fourier maps, idealized and refined using a 'riding' model, with C–H distances of 0.95 and 0.99 Å and the N–H distances of 0.88 Å, and with U_{iso} (H) = 1.2U_{eq} (CH, CH_2 and NH) or 1.5U_{eq} (CH_3).

3.2.3. Cytotoxicity testing. The cytotoxicity values of IC_{50} for the complexes **1**–**6** as well as for the ligands $\mathbf{L}_1$–$\mathbf{L}_4$ were determined by a calcein AM assay. Human cancer cell lines used were as follows: malignant melanoma (G-361), chronic myelogenous leukaemia (K-562), osteogenic sarcoma (HOS) and breast adenocarcinoma (MCF7). The technique has been previously described in greater detail.[12] After preincubation lasting 12 h at 37 °C in a 5% CO_2 atmosphere and 100% humidity, the tested compounds in the concentration range 0.2–50 μM were added. The incubation lasted 72 h and at the end of this period, the cells were incubated for 1 h with calcein AM and the fluorescence of the live cells was measured at 485/538 nm (exitation/emission) with a Fluoroskan Ascent (Labsystems). IC_{50} values, that is, the drug concentrations lethal for 50% of the tumour cells were estimated. All the experiments were repeated in triplicate with the maximal deviation 15%. All the ligands and complexes were first dissolved in DMF and then immediately diluted in water to final DMF concentration of 0.6%.

3.3. Synthesis of the complexes 1–6

3.3.1. *cis*-$[Pt(L_1)_2Cl_2]\cdot H_2O$ (1) and *cis*-$[Pt(L_2)_2Cl_2]\cdot 3H_2O$ (2). One millimole of $\mathbf{L}_1$ or $\mathbf{L}_2$ was dissolved in 10 mL ethanol and added to a mixture of *cis*-$[Pt(DMSO)_2Cl_2]$ (0.5 mmol) in 15 mL ethanol. The mixture was stirred at the room temperature for 72 h and consecutively at 50 °C for 12 h. Obtained ocher (for **1**) or white (for **2**) precipitate was filtered off, washed with ethanol (10 mL), diethylether (5 mL) and dried under an IR lamp at 40 °C. Complex **1**: Anal. Found: C, 44.3; H, 5.3; N, 16.6%. $PtCl_2C_{38}H_{52}N_{12}O_4\cdot H_2O$ requires C, 44.5; H 5.3; N, 16.4%. ES+ MS (*m*/*z*): 1007.2 [{M-(H_2O)}+H]$^+$, 1029.1 [{M-(H_2O)}+Na]$^+$, 1045.9 [{M-(H_2O)}+K]$^+$, 971.2 [{$Pt(L_1)_2Cl$}+H]$^+$, 393.4 [L_1+Na]$^+$, 371.0 [L_1+H]$^+$, 136.9 [adenine+H]$^+$. ^{1}H NMR (DMF-d_7, ppm): 9.63 (s, 1H, (O1)H), 8.47 (s, 1H, (C8)H), 8.16 (s, 1H, (N6)H), 7.18 (t, 1H, (C14)H, J = 7.7 Hz), 7.10 (s, 1H, (C11)H), 7.03 (d, 1H, (C15)H, J = 7.5 Hz), 6.80 (d, 1H, (C13)H, J = 7.9 Hz), 6.34 (s, 1H, (N2)H), 4.98 (s, 1H, (O2)H), 4.76 (d, 2H, (C9)H, J = 6.0 Hz), 4.69 (m, 1H, (C19)H), 3.96 (m, 1H, (C16)H), 3.64 (m, 1H_a (C20)H), 3.58 (m, 1H_b, (C20)H), 1.72 (sep, 1H_a, (C21)H, J = 7.1 Hz), 1.57 (d, 6H, (C17,18)H), J = 6.6 Hz), 1.47 (t, 1H_b, (C21)H, J = 7.1 Hz), 0.93 (t, 3H, (C22)H, J = 7.3 Hz). ^{13}CNMR (DMF-d_7, ppm): 160.45 (C2), 158.69 (C12), 153.60 (C6), 150.78 (C4), 141.57 (C10), 138.57 (C8), 129.95 (C11), 118.85 (C15), 115.15 (C14), 114.63 (C13), 111.31 (C5), 64.12 (C20), 55.41 (C19), 48.60 (C16), 44.81 (C9), 24.78 (C21), 21.93 (C17,18), 10.94 (C22). Complex **2**: Anal. Found: C, 44.3; H, 5.4; N, 15.6%. $PtCl_2C_{40}H_{56}N_{12}0_4\cdot 3H_20$ requires C, 44.1; H, 5.7; N, 15.4%. ES+ MS (*m*/*z*): 1035.2 [{M-($3H_2O$)}+H]$^+$, 1057.2 [{M-($3H_2O$)}+Na]$^+$, 1073.3 [{M-($3H_2O$)}+K]$^+$, 598.1 [{$Pt(L_2)$}+(H_2O)+H]$^+$, 385.2 [L_2+H]$^+$, 121.1 [purine+H]$^+$. ^{1}H NMR (DMF-d_7, ppm): 9.57 (s, 1H, (O1)H), 8.46 (s, 1H, (C8)H), 8.15 (s, 1H, (N6)H), 7.18 (t, 1H, (C14)H, J = 7.7 Hz), 7.07 (t, 1H, (C11)H, J = 1.9 Hz), 7.03 (d, 1H, (C15)H, J = 7.5 Hz), 6.78 (dd, 1H, (C13)H, J_a = 8.0 Hz, J_b = 1.7 Hz), 6.30 (d, 1H, (N2)H, J = 7.8 Hz), 4.77 (s, 1H, (O2)H), 4.75 (d, 2H, (C9)H, J = 6.0 Hz), 4.59 (t, 1H, (C19)H, J = 6.2 Hz), 3.96 (m, 1H, (C16)H), 3.66 (qui, 2H, (C20)H, J = 4.6 Hz), 2.04 (sxt, 1H, (C21)H, J = 6.8 Hz), 1.56 (dd, 6H, (C17,18)H, J_a = 6.8 Hz, J_b = 2.0 Hz), 0.95 (t, 6H, (C22,23)H, J = 5.7 Hz). ^{13}C NMR (DMF-d_7, ppm): 160.81 (C2), 158.74 (C12), 153.60 (C6), 150.79 (C4), 141.63 (C10), 138.57 (C8), 130.01 (C11), 118.87 (C15), 115.14 (C14), 114.66 (C13), 111.33 (C5), 62.63 (C20), 58.92 (C19), 48.70 (C16), 44.81 (C9), 29.00 (C21), 21.99 (C17), 21.90 (C18), 19.96 (C22), 18.91 (C23).

3.3.2. *trans*-$[Pd(L_1)_2Cl_2]\cdot H_2O$ (3) and *trans*-$[Pd(L_2)_2Cl_2]\cdot H_2O$ (4). One millimole of $\mathbf{L}_1$ or $\mathbf{L}_2$ was dissolved in 10 mL ethanol and added to a mixture of *trans*-$[Pd(DMSO)_2Cl_2]$ (0.5 mmol) in 15 mL ethanol. The mixture was stirred at the room temperature for 72 h. Afterwards, yellow (for **3**) or orange (for **4**) precipitate was formed. The solid was filtered off, washed with ethanol (10 mL), diethylether (5 mL) and dried under an IR lamp at 40 °C. Complex **3**: Anal. Found: C, 48.6; H, 5.9; N, 17.6%. $PdCl_2C_{38}H_{52}N_{12}O_4\cdot H_2O$ requires C, 48.7; H, 5.8; N, 17.9%. ES+ MS (*m*/*z*): 956.2 [[{M-(H_2O)}+K]$^+$, 917.3 [[{M-(H_2O)}+H]$^+$ 535.3 [{$Pd(L_1)Cl$}+Na]$^+$, 513.3 [{$Pd(L_1)Cl$}+H]$^+$, 393.1 [L_1+Na]$^+$, 371.2 [L_1+H]$^+$, 163.0 [9-isopropylpurine+H]$^+$, 157.1 [adenine+Na]$^+$, 136.5 [adenine+H]$^+$, 121.0 [purine+H]$^+$. ^{1}H NMR (DMF-d_7, ppm): 9.57 (s, 1H, (O1)H), 8.37 (t, 1H, (N6)H), J = 6.4 Hz), 8.18 (s, 1H, (C8)H),7.18(t,lH, (C14)H, J = 7.7 Hz), 7.10 (s, 1H, (C11)H), 7.05 (d, 1H, (C15)H, J = 7.5 Hz), 6.78 (dd, 1H, (C13)H, J_a = 8.0 Hz, J_b = 1.9 Hz), 6.32 (d, 1H, (N2)H, J = 7.5 Hz), 4.86 (s, 1H, (O2)H), 4.79 (d, 2H, (C9)H, J = 5.8 Hz), 4.69 (sep, 1H, (C19)H, J = 6.8 Hz), 3.97 (m, 1H, (C16)H), 3.65 (m, 1H_a, (C20)H), 3.58 (m, 1H_b, (C20)H), 1.74 (sep, 1H_a (C21)H) J = 6.9 Hz), 1.56 (m, 1H_b, (C21)H), 1.56 (d, 6H, (C17,18)H, J = 6.6 Hz), 0.94 (tt, 3H, (C22)H, J_a = 7.5 Hz, J_b = 2.9 Hz). ^{13}C NMR (DMF-d_7, ppm): 160.45 (C2), 158.71 (C12), 153.81 (C6), 151.30 (C4), 141.75 (CIO), 138.52 (C8), 129.98 (C11), 118.91 (C15), 115.20 (C14),

114.61 (C13), 111.85 (C5), 64.17 (C20), 55.45 (C19), 48.68 (C16), 44.85 (C9), 24.82 (C21), 21.94 (C17,18), 10.96 (C22). Complex **4**: Anal. Found: C, 49.4; H, 6.1;N, 17.1%. $PdCl_2C_{40}H_{56}N_{12}O_4{\cdot}H_2O$ requires C, 49.8; H 6.1; N, 17.4%. ES+ MS (*m*/*z*): 945.9 [{M-(H_2O)}+H]$^+$, 876.3 [{$Pd(L_2)_2$}+H]$^+$, 407.1 [L_2+Na]$^+$, 385.2 [L_2+H]$^+$, 163.0 [9-isopropylpurine+H]$^+$, 157.9 [adenine+Na]$^+$, 137.6 [adenine+H]$^+$, 121.0 [purine+H]$^+$. ^{1}H NMR (DMF-d_7, ppm): 9.56 (s, 1H, (O1)H), 8.36 (s, 1H, (C8)H), 8.17 (t, 1H, (N6)H, J = 6.4 Hz), 7.17 (t, 1H, (C14)H, J = 7.8 Hz), 7.09 (t, 1H, (C11)H, J = 2.0 Hz), 7.05 (d, 1H, (C15)H, J = 7.5 Hz), 6.77 (dd, 1H, (C13)H, J_a = 7.9 Hz, J_b = 2.0 Hz), 6.28 (d, 1H, (N2)H, J = 7.7 Hz), 4.78 (d, 2H, (C9)H, J = 5.7 Hz), 4.71 (qui, 1H, (C19)H, J = 6.8 Hz), 4.60 (t, 1H, (O2)H, J = 5.7 Hz), 3.96 (m, 1H, (C16)H), 3.66 (qui, 2H, (C20)H, J = 4.6 Hz), 2.04 (sxt, 1H, (C21)H, J = 6.8 Hz), 1.55 (dd, 6H, (C17,18)H, J_a = 6.9 Hz, J_b = 1.9 Hz), 0.95 (t, 6H, (C22,23)H, J = 6.0 Hz). ^{13}C NMR (DMF-d_7, ppm): 160.76 (C2), 158.70 (C12), 153.75 (C6), 151.28 (C4), 141.76 (C10), 138.78 (C8), 129.98 (C11), 118.87 (C15), 115.16 (C14), 114.59 (C13), 111.79 (C5), 62.63 (C20), 58.90 (C19), 48.64 (C16), 44.86 (C9), 21.97 (C17), 21.88 (C18), 19.94 (C22), 18.88 (C23).

3.3.3. *trans*-[$Pd(L_3)_2Cl_2$]·2DMF (5) and *trans*-[$Pd(L_4)_2Cl_2$]·2DMF (6). One millimole of L_3 (**5**) or L_4 (**6**) was dissolved in 10 mL ethanol and added to the mixture of K_2PdCL_4 (0.5 mmol) in 15 mL ethanol. The mixture was stirred at the room temperature for 72 h and then, yellow (for **5**) or orange (for **6**) precipitate was obtained. The solid was filtered off, washed with ethanol (10 mL), diethylether (5 mL) and dried under an IR lamp at 40 °C. The crystals suitable for X-ray analysis were obtained by the recrystallization of the complexes from DMF. Initially, *cis*-[$Pd(L_4)_2Cl_2$] (*Anal.* Found: C, 43.4; H, 4.1; N, 16.1%. $PdC_{32}H_{36}N_{10}O_4Cl_4{\cdot}(H_2O)$ requires C, 43.1; H 4.3; N, 15.7%) was prepared, but after the recrystallization from DMF, it was transformed into *trans*-[$Pd(L_4)_2Cl_2$]·2DMF (see Section 2.6.). Complex **5**: Anal. Found: C, 45.0; H, 4.9; N, 17.5%. $PdC_{30}H_{32}N_{10}O_2Cl_4{\cdot}(C_3H_7NO)_2$ requires C, 45.1; H 4.8; N, 17.5%. ES+ MS (*m*/*z*): 763.7 [{$Pd(L_3)_2$}+Na]$^+$, 742.9 [{$Pd(L_3)_2$}+H]$^+$, 340.1 [L_3+Na]$^+$, 318.1 [L_3+H]$^+$, 121.0 [purine+H]$^+$. ^{1}H NMR (DMF-d_7, ppm): 9.58 (s, 1H, (O1)H), 8.95 (t, 1H, (N6)H, J = 5.9 Hz), 8.86 (s, 1H, (C8)H), 7.16 (t, 1H, (C14)H, J = 7.9 Hz), 7.04 (t, 1H, (C11)H, J = 1.9 Hz), 7.00 (d, 1H, (C15)H, J = 7.5 Hz), 6.77 (dd, 1H, (C13)H, J_a = 7.9 Hz, J_b = 2.2 Hz), 4.87 (sep, 1H, (C16)H, J = 6.8 Hz), 4.87 (d, 2H, (C9)H, J = 6.0 Hz), 1.61 (d, 6H, (C17,18)H, J = 6.8 Hz). ^{13}C NMR (DMF-d_7, ppm): 158.79 (C2), 155.15 (C12), 154.16 (C6), 150.20 (C4), 143.17 (C8), 140.44 (C10), 130.06 (C11), 118.80 (C15), 116.72 (C5), 115.17 (C14), 114.86 (C13), 49.97 (C16), 45.39 (C9), 22.07 (C17,18). Complex **6**: Anal. Found: C, 44.9; H, 4.9; N, 16.9%. $PdC_{32}H_{36}N_{10}O_4Cl_4{\cdot}(C_3H_7NO)_2$ requires C, 44.7; H 4.9; N, 16.5%. ES+ MS (*m*/*z*): 912.0 [M+K]$^+$, 819.6 [{$Pd(L_4)_2$}+(H_2O)+H]$^+$, 803.7 [{$Pd(L_4)_2$}+H]$^+$, 386.0 [L_4+K]$^+$, 370.0 [L_4+Na]$^+$, 348.1 [L_4+H]$^+$, 121.0 [purine+H]$^+$. ^{1}H NMR (DMF-d_7, ppm): 9.13 (s, 1H, (O1)H), 8.99 (t, 1H, (N6)H, J = 6.1 Hz), 8.84 (s, 1H, (C8)H), 7.11 (dd, 1H, (C15)H, J_a = 7.8 Hz, J_b = 1.2 Hz), 6.94 (dd, 1H, (C13)H, J_a = 7.9 Hz, J_b = 1.2 Hz), 6.74 (t, 1H, (C14)H, J = 7.9 Hz), 4.98 (d, 2H, (C9)H, J = 6.1 Hz), 4.90 (sep, 1H, (C16)H, J = 6.8 Hz), 3.86 (s, 3H, (C19)H), 1.63 (d, 6H, (C17,18)H, J = 6.8 Hz). ^{13}C NMR (DMF-d_7, ppm): 155.16 (C2), 154.22 (C6), 150.16 (C4), 148.46 (C12), 145.28 (C11), 143.07 (C8), 125.28 (C10), 120.91 (C15), 119.46 (C14), 116.73 (C5), 111.57 (C13), 56.37 (C19), 50.05 (C16), 40.88 (C9), 22.03 (C17,18).

4. Conclusion

A series of complexes of the types *cis*-[$Pt(L)_2Cl_2$] and *trans*-[$Pd(L)_2Cl_2$], where L = CDK inhibitor derived from 6-benzylamino-9-isopropylpurine, have been synthesized and characterized. The molecular structures of CDK inhibitor, used as ligand L_1, and the *trans*-Pd(II) complexes **5** and **6** have been determined by a single crystal X-ray analysis. The square-planar geometry as well as the *trans*-arrangement in the vicinity of the central palladium atom has been proved unambiguously. It consists of a PdN_2Cl_2 chromophore, constituted of two organic ligands bonded via N(7) of the imidazole ring and of two chlorides. The best IC_{50} values, 6 and 6 μM against G-361 and HOS, respectively, were obtained for the complex **1**, and are much lower than the values obtained for the initial ligand L_1. These results are very promising because the IC_{50} values for the complex **1** are of the same order as the values obtained for *Cisplatin* and even better than the values achieved for *Oxaliplatin*. The IC_{50} values of the complexes **3** and **4** against MCF7 and K-562 are 3 μM 7 μM for **3** and 3 and 6 μM for **4**, which is higher by order of magnitude in comparison with the cytotoxicity of the starting ligands, and, surprisingly, much better than the values achieved for *Cisplatin* and *Oxaliplatin*.

5. Supplementary material

Crystallographic data for the structures reported in this paper have been deposited with the Cambridge Crystallographic Data Centre as supplementary publication Nos. CCDC 268241 (for L_1), 268242 (for **5**) and 268243 (for **6**). Copies of the data can be obtained, free of charge, on application to CCDC, 12 Union Road, Cambridge CB2 1EZ, UK; fax: +44-1223-336-033, e-mail: deposit@ccdc.cam.ac.uk; http//www.ccdc.cam.ac.uk.

Acknowledgments

This research was supported by the Ministry of Education, Youth and Sports (MSM6198959218) and by the Grant Agency of the Czech Republic (Grant No. 203/04/1168). The authors thank Dana Vychodilová for elemental analyses and IR spectra measurements, Ondřej Novák for obtaining of ES+ MS spectral data, Michal Maloň for ^{195}Pt NMR spectra measurements, Libor

Machala for his help with acquiring of the thermal analyses data and Eva Hirnerová for cytotoxicity testing.

References and notes

1. Kelland, L. R.; Sharp, S. Y.; O'Neil, C. F.; Raynaud, F. I.; Beale, P. J.; Judson, I. R. *J. Inorg. Biochem.* **1999**, *77*, 111.
2. Hambley, T. W. *Coord. Chem. Rev.* **1997**, *166*, 181.
3. Barefoot, R. R. *J. Chromatogr. B* **2001**, *751*, 205.
4. Harrap, K. R. *Cancer Res.* **1995**, *55*, 2761.
5. Extra, J. M.; Espic, M.; Calvo, F.; Ferme, C.; Mignot, L.; Marty, M. *Cancer Chemother. Pharmacol.* **1990**, *25*, 299.
6. Natile, G.; Coluccia, M. *Coord. Chem. Rev.* **2001**, *216–217*, 383.
7. Tessier, Ch.; Rochon, F. D. *Inorg. Chim. Acta* **1999**, *295*, 25.
8. Thompson, LK. *Inorg. Chim. Acta* **1980**, *38*, 117.
9. Kong, P.-Ch.; Rochon, F. D. *Inorg. Chem. Acta* **1981**, *61*, 269.
10. Budzisz, E.; Malecka, M.; Nawrot, B. *Tetrahedron* **2004**, *60*, 1749.
11. Gökçe, M.; Utku, S.; Gür, S.; Özkul, A.; Gümüş, F. *Eur. J. Med. Chem.* **2005**, *40*, 135.
12. Trávníček, Z.; Maloň, M.; Zatloukal, M.; Doležal, K.; Strnad, M.; Marek, J. *J. Inorg. Biochem.* **2003**, *94*, 307.
13. Pneumatitakis, G.; Hadjiliadis, N.; Theophanides, T. *Inorg. Chem.* **1978**, *17*, 915.
14. Quirós, M.; Salas, J. M.; Sánches, M. P. *Inorg. Chim. Acta* **1993**, *204*, 213.
15. Szłyk, E.; Grodzicki, A.; Pazderski, L.; Wojtczak, A.; Chatłas, J.; Wrzeszcz, G.; Sitkowski, J.; Kamieński, B. *J. Chem. Soc. Dalton Trans.* **2000**, 867.
16. Farrell, N.; Povirk, L. F.; Dange, Y.; DeMasters, G.; Gupta, M. S.; Kohlhagen, G.; Khan, Q. A.; Pommier, Y.; Gewirtz, D. A. *Biochem. Pharmacol.* **2004**, *68*, 857.
17. Farrell, N.; Ha, T. T. B.; Souchard, J.-P.; Wimmer, F. L.; Cros, S.; Johnson, N. P. *J. Med. Chem.* **1989**, *32*, 2241.
18. Skoog, F.; Hamzi, H. G.; Szweykowska, A. M.; Leonard, N. J.; Carraway, K. L.; Fujii, T.; Helgeson, J. P.; Loeppky, R. N. *Phytochemistry* **1967**, *6*, 1169.
19. Veselý, J.; Havlíček, L.; Strnad, M.; Blow, J. J.; Donella-Deana, A.; Pinna, L.; Letham, D. S.; Kato, J.; Detivaud, L.; Leclerc, S. *Eur. J. Biochem.* **1994**, *224*, 771.
20. Moravec, J.; Kryštof, V.; Hanuš, J.; Havliček, L.; Moravcová, D.; Fuksová, K.; Kuzma, M.; Lenobel, R.; Otyepka, M.; Strnad, M. *Bioorg. Med. Chem. Lett.* **2003**, *13*, 2993.
21. Havlíček, L.; Hanuš, J.; Veselý, J.; Leclerc, S.; Meijer, L.; Shaw, G.; Strnad, M. *J. Med. Chem.* **1997**, *40*, 408.
22. Kryštof, V.; Lenobel, R.; Havliček, L.; Kuzma, M.; Strnad, M. *Bioorg. Med. Chem. Lett.* **2002**, *12*, 3283.
23. Maloň, M.; Trávníček, Z.; Maryško, M.; Marek, J.; Doležal, K.; Rolčík, J.; Strnad, M. *Trans. Met. Chem.* **2002**, *27*, 580.
24. Trávníček, Z.; Maloň, M.; Biler, M.; Hajdúch, M.; Brož, P.; Doležal, K.; Holub, J.; Kryštof, V.; Strnad, M. *Trans. Met. Chem.* **2000**, *25*, 265.
25. Trávníček, Z.; Maloň, M.; Popa, I.; Doležal, K.; Strnad, M. *Trans. Met. Chem.* **2002**, *27*, 918.
26. Trávníček, Z.; Klanicová, A.; Popa, I.; Rolčík, J. *J. Inorg. Biochem.* **2005**, *99*, 776.
27. Geary, W. J. *Coord. Chem. Rev.* **1971**, *7*, 81.
28. Lock, C. J.; Zvagulis, M. *Inorg. Chem.* **1981**, *20*, 1817.
29. Kong, P.-Ch.; Rochon, F. D. *Inorg. Chim. Acta* **1984**, *83*, 65.
30. Harris, R. K.; Mann, F.; Kidd, R. G.; Goodfellow, R. J. *NMR and the Periodic Table*; Academic Press: London, p 250.
31. Pregosin, P. S. *Transition Metal Nuclear Magnetic Resonance*; Elsevier: Amsterdam, 1991, p 228.
32. Łakomska, I.; Szłyk, E.; Sitkowski, J.; Kozerski, L.; Wietrzyk, J.; Pełczyńska, M.; Nasulewicz, A.; Opolski, A. *J. Inorg. Biochem.* **2004**, *98*, 167.
33. Pouchert, C. J. *The Aldrich Library of Infrared Spectra*, third ed.; Aldrich Chemical Company Press: Milwaukee, 1981.
34. Nakamoto, K. *Infrared and Raman Spectra of Inorganic and Coordination Compounds Part B: Applications in Coordination, Organometallic and Bioinorganic Chemistry*, fifth ed.; Wiley: New York, 1991.
35. Durig, J. R.; Layton, R.; Sink, D. W.; Mitchell, B. R. *Spectrochim. Acta* **1965**, *21*, 1367.
36. DSC XP-10,Ver. 3.3.0.7 (*D*), THASS, **2003**.
37. Maloň, M.; Trávníček, Z.; Maryško, M.; Zbořil, R.; Mašláň, M.; Marek, J.; Doležal, K.; Rolčik, J.; Kryštof, V.; Strnad, M. *Inorg. Chim. Acta* **2001**, *323*, 119.
38. Raghunathan, S.; Sinha, B. K.; Pattabhi, V.; Gabe, E. *J. Acta Cryst.* **1983**, *C39*, 1545.
39. Trávníček, Z.; Popa, I.; Doležal, K. *Acta Cryst.* **2004**, *C60*, 662.
40. Trávníček, Z.; Kryštof, V. *Acta Cryst.* **2004**, *E60*, 2324.
41. Sheldrick, G. M. SHELXL 97, Program for crystal structure refinement. University of Göttingen, Göttingen: Germany, 1997.
42. Allen, F. H. *Acta Cryst.* **2002**, *B58*, 380.
43. Price, C.; Shipman, M. A.; Rees, N. H.; Elsegood, M. R. J.; Edwards, A. J.; Clegg, W.; Houlton, A. *Chem. Eur. J.* **2001**, *7*, 1194.
44. Price, J. H.; Williamson, A. N.; Schamm, R. F.; Wayland, B. B. *Inorg. Chem.* **1972**, *11*, 1280.
45. Khodadad, P.; Ceolin, R. *Therm. J. Analysis* **1985**, *30*, 1141.
46. Oxford Diffraction, *CrysAlis RED* and *CrysAlis CCD* software (Ver. 1.171.23), Oxford Diffraction Ltd., Abingdon, Oxfordshire, England 2003.
47. Sheldrick, G. M. *SHELXS 97 Acta crystallogr. A* **1990**, *46*, 467.